2013 European Control Conference (ECC)
July 17-19, 2013, Zürich, Switzerland.

Robust control of magnetic guidance lightweight AGVs path tracking using randomization methods

M. G. Madaschi[1], E. Gryazina[2], A. L. Cologni[1], C. Spelta[1], F. Previdi[1], S. M. Savaresi[3], I. Pesenti[4]

Abstract— **In this paper, a state space dynamical model for the differential drive path tracking system of an AGV (Automated Guided Vehicle) is developed. In order to guarantee desirable control specifications for a wide range of possible masses ($50 < M < 1000kg$), the payload mass is considered as uncertainty in the model. Robust stability domain in the controller parameter space via randomization technique is analysed. Two sets of controller parameters are selected and experimentally tested on a commercial vehicle, showing performances in agreement with the analysis.**

I. INTRODUCTION

Nowadays AGVs are used in many production environments and warehouses such as the automotive industry, logistics or container harbours. In general, these devices are highly expensive and often not flexible, mainly due to their large dimensions and weight. In fact, they are designed to move loads whose weight is not too large in comparison with the vehicle weight. So, they are not used in small or medium size enterprises, where the investment cost could have a high impact on the cost structure of the handled products or the warehouse dimensions are reduced. In this paper, a light AGV developed by Scaglia Indeva S.p.A. (Brembilla, Italy) is presented. Light AGVs are usually designed to move small payloads and their distinctive feature is their high flexibility and reconfigurability in the load handling. However, they have usually limited load weight capacity. In fact, large load weight values have a high impact on the guidance performances, even affecting the vehicle mechanical stability and strong speed limitations are usually applied. Moreover, when designed to move loads in a large range of weight values, from small light plastic objects to heavy metal components, the performance are conservatively chosen on the basis of the largest expected payload. So, in this work, we focused our attention to the vehicle guidance control problem and aim to design controllers that guarantees desirable specifications for a wide range of possible load mass values. Hence, we assume that the payload mass is an uncertainty in the model and resort to robust control design methods. Moreover, we'd like not only to find one suitable controller but to analyze the stability domain in the controller parameter space, so that we can evaluate the effects on the guidance performances produced by changes in the controller parameters, preserving control system stability. In order to obtain such results we pay special attention to randomized techniques. The variety of randomized algorithms for control can be found in [1]; special techniques for fixed order controller design are described in [2], [3]; the problem of static output control feedback is discussed in [4]. We prefer this parameter space approach because it allows not only to compute controller parameters but also to compute a discrete set of stabilizing controllers and to obtain a configuration of the admissible domain in the parameter space. Moreover, it is demonstrated in [3] how randomized techniques are oriented to deal with basic notions for any engineering characteristics — gain or phase margin, overshoot or other time-response characteristics, robustness margin — as well as mathematical objectives such as H_2 or H_∞ norm. Specifically, randomized method are applied to the tuning of PI controllers [5], taking into account control action limitations, due to the limited current supply values; system speed specifications, defined by desired values for settling time; H_∞ performances. The controller performances have been tested on an AGV used on a commercial vehicle engines assembly line. In Sect. II the layout of the vehicle is described looking at sensors, actuators and guidance system architecture. Then, a complete dynamical model of the system is developed, in order to perform robust control design. As an output of the modelling stage, the control system architecture is described in Sect. III, where the MIMO system is decoupled by means of a static matrix gain applied to the left and right DC brushless motor current. Then in Sect. IV we analyze the robustly stabilizing controllers and take two for experimental tests that are described in Sec. V.

II. EXPERIMENTAL SETUP AND VEHICLE DYNAMICS MODEL

A. Vehicle description

An Automatic Guided Vehicle (AGV) is a wheeled mobile robot used to move materials inside a production site. The AGV considered in this work is a prototype designed by Scaglia Indeva S.p.A. Italy and it is a Wheeled Mobile Robot (WMR) with two independent drive wheels placed in the middle of the vehicle chassis, two pivoting wheels in the front and two fixed wheels in the rear. Pivoting and fixed wheels are used to guarantee mechanical stability (see Fig. 1 and Fig. 2).

The vehicle considered in this paper is a magnetic guidance AGV. A magnetic strip is placed on the floor to define the vehicle course. The magnetic strip considered in this

This work was supported in part by Scaglia-Indeva S.p.A. and Landau Network - Centro Volta

[1]Dipartimento di Ingegneria, Università di Bergamo Dalmine (BG), Italy matteo.madaschi@unibg.it

[2]Institute of Control Sciences, Russian Academy of Sciences 65 Profsoyuznaya str., 117997 Moscow, Russia

[3]Dipartimento di Elettronica e Informazione, Politecnico di Milano, Milano, Italy

[4]R&D Business Unit, Scaglia−Indeva S.p.A. via Marconi, 42 − 24012 Brembilla (BG), Italy

Fig. 1. AGV prototype

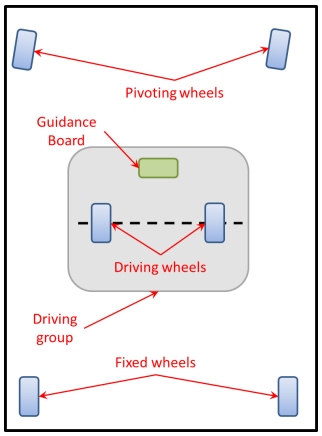

Fig. 2. Top view scheme of the AGV

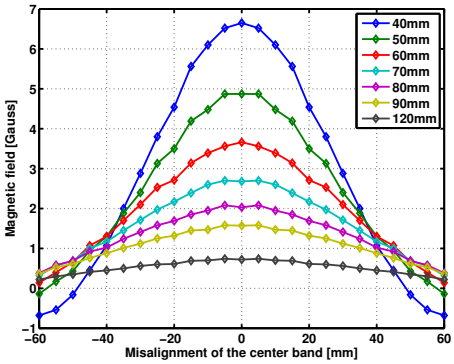

Fig. 3. Magnetic intensity strength in vertical position

work is 5cm wide, and the magnetic field intensity is shown in Fig. 3. The relative position of the vehicle with respect to the strip is estimated with the use of three sensors dedicated to measure the field intensity. These sensors are mounted on the Guidance Electronic Board, positioned in the front part of the steering group.

The AGV is equipped with two very compact and powerful DC brushless electric motors: the AGV can move loads up to 1000Kg at the maximum speed (50m/min).

In order to control the vehicle an ECU Board with a microcontroller is used: it is connected to the Guidance Electronic Board through a CAN connection.

B. Vehicle Dynamic Model

The vehicle can be modeled considering, first, the kinematic model of the differential drive as shown in Fig. 4. As well known, in the considered framework it is possible to describe the vehicle kinematic using only two variables [6]

- the speed $\bar{v}$, tangent to the vehicle trajectory;
- the angular speed $\dot{\vartheta}$, representing the rotation of the vehicle around the Instantaneous Center of Rotation (ICR);

Being (Fig. 4):

- l the distance between the driving wheels;

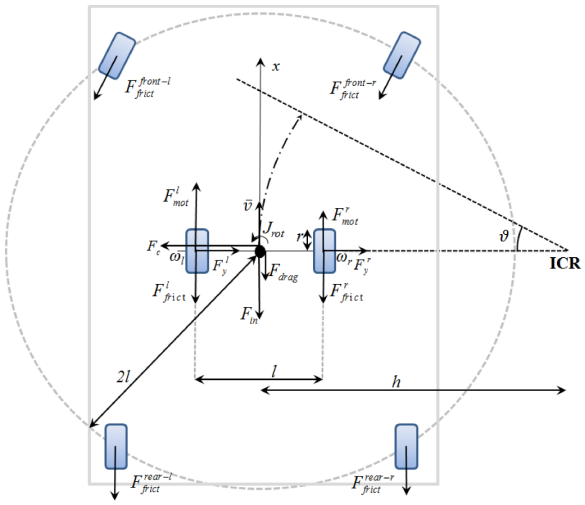

Fig. 4. Kinematic and forces on the considered vehicle

- r the driving wheel radius (assumed equal for both wheels);
- h the distance between O (the midpoint of the vehicle axis) and the ICR;

Accordingly, in the hypothesis that no wheel slip occurs, the tangent speed $\bar{v}$ and the angular speed $\dot{\vartheta}$ are:

$$\begin{cases} \bar{v} = \dfrac{\omega_l + \omega_r}{2} r \\ \dot{\vartheta} = \dfrac{\omega_l - \omega_r}{l} r \end{cases} \tag{1}$$

where ω_l and ω_r are the rotational speed of the left and the right wheels, respectively, which are measured variables for the considered vehicle. Furthermore, h can be expressed as $h = \frac{l}{2}(\omega_l + \omega_r)/(\omega_l - \omega_r)$.

In order to control the vehicle it is necessary to derive a control oriented model, having in mind that the physical control inputs for the system are the two motor currents, which will be regulated by the inverters, while the controlled variables are

$$\begin{cases} \bar{\omega} = \dfrac{\omega_l + \omega_r}{2} = \dfrac{\bar{v}}{r} \\ \Delta\omega = \omega_l - \omega_r = \dot{\vartheta}\dfrac{l}{r} \end{cases} \tag{2}$$

The variables $\bar{\omega}$ and $\Delta\omega$ in (2) represent the *vehicle longitudinal speed* and the *steering speed*, respectively. Coherently with such choice, the control variables are defined as $\bar{i} = (i^l_{mot} + i^r_{mot})/2$ and $\Delta i = i^l_{mot} - i^r_{mot}$ where i^l_{mot} and i^r_{mot} represent the input current of the left and right motor, respectively.

Once both control and controlled variables have been defined, the Input/Output system dynamics can be described by the following MIMO model

$$\begin{bmatrix} \bar{\omega} \\ \Delta\omega \end{bmatrix} = \begin{bmatrix} G_{11}(s) & G_{12}(s) \\ G_{21}(s) & G_{22}(s) \end{bmatrix} \begin{bmatrix} \bar{i} \\ \Delta i \end{bmatrix} \tag{3}$$

where $G_{11}(s)$, $G_{12}(s)$,$G_{21}(s)$, $G_{22}(s)$ are suitable transfer functions. Now, consider the schematic view given in Fig. 4, where

- J_{rot} is the rotational inertia of the vehicle;
- F_{in} is the inertial force;
- F_c is the centrifugal force;
- F_{ly} and F_{ry} are the lateral forces acting on the left and right driving wheels;
- $F_{frict}^{front-l}$ and $F_{frict}^{front-r}$ are the friction forces acting on the pivoting wheels;
- F_{frict}^{rear-l} and F_{frict}^{rear-r} are the friction forces acting on the left and right drag wheels;
- F_{frict}^{l} and F_{frict}^{r} are the friction forces acting on the left and right driving wheels
- F_{drag} is the aerodynamic drag force acting on the vehicle;
- F_{mot}^{l} and F_{mot}^{r} are the traction forces provided by the electric motors;
- M is the mass of the vehicle;

The wheel radius r is assumed equal for pivoting, drag and driving wheels. The center of mass is supposed to be coincident with the axis midpoint O. The vehicle chassis can be modeled as a parallelepiped. The vehicle is considered as a rigid body moving on the plane with two degrees of freedom, since it can be supposed that, in normal operation, the centrifugal forces are always balanced by the lateral friction: $F_c = F_y^l + F_y^r$

The friction forces acting on the vehicle are:

- The rolling resistance $F_{roll} = C_{roll} Mg$
- The dynamic viscous resistance $F_{dyn}(\bar{v}) = \beta_{dyn}\bar{v}$
- The aerodynamic drag force $F_{drag}(\bar{v}) = \frac{1}{2}\rho c_v A(\bar{v} + v_{wind})^2$

where:

- C_{roll} is the rolling coefficient;
- β_{dyn} is the dynamic viscous resistance coefficient;
- ρ is the density of the air;
- c_v is the drag coefficient;
- A is the reference front vehicle area;
- v_{wind} is the speed of the wind.

So the total friction force can be represented by the following equation:

$$F_{frict}(\bar{v}) = C_{const} + C_{prop}\bar{v} + C_{quad}\bar{v}^2 \tag{4}$$

Since in normal operating conditions the vehicle maximum speed is 3km/h and it is used indoor, it is possible to omit the quadratic term in (4). Accordingly, the friction forces for the driving wheels can be expressed as follows:

$$F_{frict}^{i}(\omega_i) = C_{const}^{i} + C_{prop}^{i}\omega_i r, \;\; i = l, r \tag{5}$$

In order to estimate the parameters of (5), coasting down experiments have been carried out by letting the system inertially decelerate from its maximum nominal speed (3km/h) to zero. The estimated parameters are listed in Table I Since $C_{const}^{l} \cong C_{const}^{r}$ it is possible to use a single parameter C_{const} in the following.

As a final remark on wheel parameters estimation, it is worth noting that, introducing aerodynamical friction in the model, the corresponding drag coefficient estimated by coasting down experiments is negligible for all tests.

TABLE I

COEFFICIENTS FROM COASTING-DOWN FRICTION IDENTIFICATION

	$C_{const}\ [N]$	$C_{prop}\ [Ns/m]$
Left wheel	6.371	16.096
Right wheel	6.432	16.245

Now, let's write the force balance along the vehicle longitudinal x axis:

$$\Sigma F^x = F_{in}^x + F_{frict}^x - F_{mot}^x = 0 \tag{6}$$

where

$$F_{mot}^x = \frac{\eta n k}{r}\left(i_{mot}^l + i_{mot}^r\right) = \frac{2\eta n k}{r}\bar{i} \tag{7}$$

$$F_{frict}^x(\bar{v}) = \left(C_{prop}^l + C_{prop}^r\right)\bar{v} + \left(C_{prop}^r - C_{prop}^l\right)\Delta v + 2C_{const} \tag{8}$$

and

$$F_{in}^x = \left(M + \frac{2J_p}{r^2} + \frac{J_{mot}\eta}{r^2 n^2} + 2M_w + \frac{2J_{pivot}}{r^2}\right)\dot{\bar{\omega}} r \tag{9}$$

where

- J_{pivot} is the inertia of each pivoting wheel;
- η is the gearbox efficiency;
- n is the gearbox reduction ratio;
- k is torque constant;
- J_p is the inertia of vehicle;
- M_w is the mass of each fixed wheel

Notice that in (9), M, the total mass vehicle, is a largely dominant addendum with respect to the other and so (9) can be strongly simplified as $F_{in}^x = M\dot{\bar{\omega}} r$.

Thus, (6) takes the form

$$\begin{aligned} &M\dot{\bar{\omega}} r + \left(C_{prop}^l + C_{prop}^r\right)\bar{v} + \\ &\left(C_{prop}^r - C_{prop}^l\right)\Delta v + 2C_{const} = \frac{2k\eta n\bar{i}}{r} \end{aligned} \tag{10}$$

Now, consider the torque balance around the center of mass of the vehicle, which can be described as follows:

$$\Sigma T^{(O)} = \Sigma T_{in}{}^{(O)} + \Sigma T_{frict}{}^{(O)} - \Sigma T_{driving}{}^{(O)} = 0 \tag{11}$$

The inertia torque is given by $\Sigma T_{in}{}^{(O)} = J_{rot}\ddot{\vartheta}$.

The driving torque, according to the convention adopted in Fig. 4, can be calculated as

$$\begin{aligned} \Sigma T_{driving}{}^{(O)} &= \frac{l}{2}\left(F_{mot}^l - F_{mot}^r\right) \\ &= \frac{l}{2}\frac{\eta n k}{r}\left(i_{mot}^l - i_{mot}^r\right) \end{aligned} \tag{12}$$

The friction torque ΣT_{frict}^{O} has the form

$$\Sigma T_{frict}{}^{(O)} = \frac{l}{2}\left(F_{frict}^l - F_{frict}^r\right) + bF_{frict}^{pivot-rear} \tag{13}$$

Since $C_{rear}, C_{pivot} \ll \frac{C_{prop}^l + C_{prop}^r}{2}$ and ϑ is a small angle in normal operations, the last term in (13) representing the

friction forces due to pivoting and fixed wheels can be neglected. Thus, (11) takes the form

$$\begin{aligned} & J_{rot}\frac{r}{l}\Delta\dot{\omega}+\frac{lr}{4}\left(C^l_{prop}+C^r_{prop}\right)\Delta\omega \\ & +\frac{lr}{2}\left(C^l_{prop}-C^r_{prop}\right)\bar{\omega}+\frac{l}{2}\left(C^l_{\mathrm{const}}-C^r_{const}\right) \\ & =\frac{l}{2}\frac{\eta nk}{r}\Delta i \end{aligned} \tag{14}$$

Finally, the state equations of the model are

$$\begin{cases} \dot{\bar{\omega}}=-\dfrac{\left(C^l_{prop}+C^r_{prop}\right)}{M}\bar{\omega}-\dfrac{\left(C^r_{prop}-C^l_{prop}\right)}{2M}\Delta\omega \\ \quad -\dfrac{2C_{\mathrm{const}}}{Mr}+\dfrac{2k\eta n}{Mr^2}\bar{i} \\ \Delta\dot{\omega}=-\dfrac{l^2}{2J_{rot}}\left(C^r_{prop}-C^l_{prop}\right)\bar{\omega}-\dfrac{l^2}{4J_{rot}}\left(C^l_{prop}+C^r_{prop}\right)\Delta\omega \\ \quad -\dfrac{l^2}{2rJ_{rot}}\left(C^l_{\mathrm{const}}-C^r_{const}\right)+\dfrac{l}{2}\dfrac{\eta nk}{r}\Delta i \end{cases} \tag{15}$$

The output equation is

$$y=\begin{bmatrix} y_1 \\ y_2 \end{bmatrix}=\begin{bmatrix} 1 & 0 \\ 0 & 1 \end{bmatrix}\begin{bmatrix} \bar{\omega} \\ \Delta\omega \end{bmatrix} \tag{16}$$

Since **B** and **C** matrices are diagonal, with reference to (3), the off-diagonal transfer functions $G_{12}(s)$ and $G_{21}(s)$ are zero and so the system is decoupled, i.e. the 2x2 MIMO system is simply made by two SISO systems. Finally, remembering that $C_{const}=C^l_{const}\cong C^r_{const}$ and $C_{prop}=C^l_{prop}\cong C^r_{prop}$, all the friction coefficients for the left and right wheels can be assumed equal. Therefore,the state equations become

$$\begin{cases} \dot{\bar{\omega}}=-\dfrac{C_{app}}{M}\bar{\omega}-\dfrac{2C_{\mathrm{const}}}{Mr}+\dfrac{2k\eta n}{Mr^2}\bar{i} \\ \Delta\dot{\omega}=-\dfrac{l^2C_{app}}{2J_{rot}}\Delta\omega+\dfrac{l}{2}\dfrac{\eta nk}{r}\Delta i \end{cases} \tag{17}$$

III. VEHICLE MOTION CONTROL ARCHITECTURE

As shown in Fig. 5 the control system is composed by two nested control loops: a servo-controller for motor currents and an external loop that regulates vehicle speed and steering speed as defined in (2). The current control loops are embedded in the inverters that feed the DC brushless motors and they are designed to ensure the frequency decoupling with the mechanical outer loop. The mechanical control loops are driven by two set-points: the desired longitudinal speed $\bar{\omega}^*$ provided by user and desired steering speed $\Delta\omega^*$ provided by Guidance Electronic Board that computes it on the basis of the strip reading.

IV. PARAMETER ANALYSIS FOR CONTROLLER DESIGN

In this Section, randomized techniques are used to evaluate the stability domain in the parameter controller space. Randomized techniques are of particular interest in applications. In fact, they are oriented to deal in an immediate and intuitive

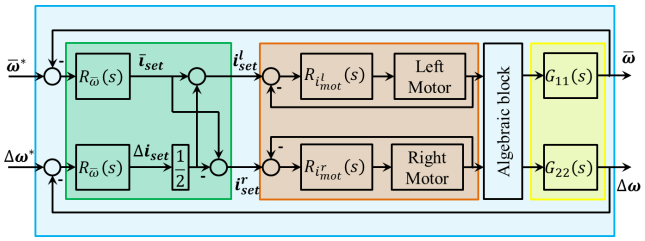

Fig. 5. Decoupled control layout for the considered AGV

way with basic control engineering design parameters, such as gain or phase margins, time-response characteristics. But they can accommodate as well also mathematical objectives such as H_2 or H_∞ norm. Specifically, in the present application, a PI controller [5] is considered, which is a very simple controller with only two parameters. In this way, the controller parameter analysis will be represented by two-dimensional plots. This will provide a very simple interpretation of the results obtained by application of randomized techniques. The first step is to generate samples in the stability (or robust stability) domain, i.e. to find controller parameter values (robustly) stabilizing the plant. In general, the geometry of this domain can be quite complicated [7], but sampling allows to overcome this difficulty. In the following, first the sampling method for the stability domain is described and the robust stability domain with respect to mass variation is depicted. Then, the control action constraints (current limitations) and the performance requirements (transient time duration) are shown in the stability domain. Finally, also H_∞ norm constraints are shown in the same picture, merging robustness, performance and constraint requirements in a single analysis, simple and easy to understand.

A. Sampling for stability domain for polynomials

Consider a LTI SISO plant $G(s)=\frac{h(s)}{e(s)}$. We wish to stabilize it with the controller $C(s)=\frac{f(s)}{g(s)}$ where polynomials $f(s),g(s)$ have fixed orders (for instance, as in the case of the present application, it can be a PI controller). The closed-loop characteristic polynomial of the system is linear in the controller parameters, given by the vector k, whose dimension is equal to the number of controller parameters so that: $p(s)=h(s)f(s)+e(s)g(s)=p_0(s)+\sum_{i=1}^{n}k_ip_i(s)$. Suppose that at least one stabilizing controller is known, with parameter vector k^0 such that $p(s,k^0)$ is stable. Our aim is to generate samples k^i that are asymptotically uniform in the stability domain. To achieve this goal we apply the Hit-and-Run algorithm [8]. At every step, the algorithm generates a random direction uniformly sampled among all directions and then it chooses the next point by uniform sampling over the segment of the line along the chosen direction and inside the stability domain.

Let d be a random direction uniformly chosen in the unit sphere in $\mathbb{R}^n$, n being the controller parameter space dimension, in order to specify the segment of the line d in the stability domain, namely, the values $L=\{t\in\mathbb{R}:$

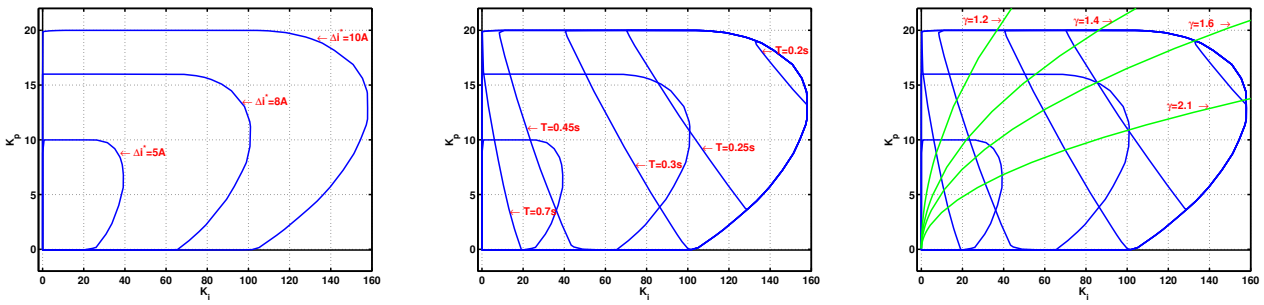

(a) (b) (c)

Fig. 6. Robust stability domain $\mathscr{K}_0$ with: (a) domains of maximal admissible $\Delta i^* = [5,8,10]A$, (b) level sets of transient time for $T = [0.2, 0.25, 0.3, 0.45, 0.7]$s and (c) $||T||_\infty \leq \gamma$ with $\gamma = [1.2, 1.4, 1.6, 2.1]$.

$p(s,k^0) + t\sum d_i p_i(s)$is stable$\}$

It is necessary to solve the stability analysis problem for a SISO system with a real scalar gain. This problem can be analytically solved [7]Then, a new sample $k^1 = k^0 + \tau d$ is chosen, where τ is uniform random in L. Finally, k^0 is replaced with k^1 and the procedure is repeated to obtain an arbitrary large number of samples $k^0, k^1, \ldots, k^N$.

A similar procedure can be applied to sample for robust stability domain for interval plant $G(s) = \frac{h(s,q)}{e(s,q)}$, $\underline{q} \leq q \leq \overline{q}$ (see [9] for details).

Further on, in this Section, we describe how randomized techniques can be exploited to choose the controller parameters taking into account several control objectives. Specifically, we focus our attention on the second equation in (17), describing the steering speed control with the aim of designing a PI controller.

B. Robust stability domain

The transfer function from current Δi to steering speed $\Delta\omega$ depends on the mass value M and has the following form

$$G(s) = \frac{260.26}{Ms + 17.18}$$

We are looking for PI controllers $C(s) = k_p + \frac{k_i}{s}$ stabilizing the system for all mass values $50 \leq M \leq 1000$. In this case the precise robust stability domain description, obtained by D-decomposition technique, is:

$$\mathscr{K}_0 = \{k_i > 0, k_p > -0.066\}.$$

Note that mathematically robust stability domain is not bounded but practically we are unable to realize controller with arbitrary large gains k_p and k_i. Moreover, performance specifications on the controlled system dynamical behaviour must be fulfilled and expressed as constraints in the controller parameter space.

C. Limitations on control action

The control input $\Delta i < \Delta i^*$ value is restricted by 10 A. This constraint naturally makes the stability parameter domain bounded. To estimate the feasible set we put 10000 samples in the domain $0 < k_i < 160$, $-0.066 < kp < 50$ and calculate $\max \Delta i$ needed to realize such a controller. In Fig. 6(a) the domains for different maximum admissible Δi are plotted. As a consequence of this analysis, we restrict the controller parameter values to $0 < k_i < 158$, $-0.066 < k_p < 20$.

D. Controlled system speed performance requirements

In practice, specification on the system speed are often given as limitations on the step response transient time value. Again, using sampling, 10000 uniform random samples are taken in the controller parameter domain and the regions are plotted such that the transient time τ is so that $\tau \leq T$, $T = [0.2,\ 0.25,\ 0.3,\ 0.45,\ 0.7]s$. The transient time is calculated for the largest possible mass value, i.e. $M = 1000$kg, hence, smaller transient time for smaller masses is guaranteed. Fig. 6(b) depicts level sets for various transient time. Notice that when we restrict ourselves with $\Delta i < 8$A it is possible to choose a controller such that transient time remains below 0.25s. When we increase upper bound for Δi to 10A it becomes possible to achieve transient time 0.2s.

E. H_∞ performance evaluation

Now we want to take into account H_∞ performance. The paper [10] shows how the domains in controller parameter space such that $||T(s,k_i,k_p)||_\infty \leq \gamma$ can be efficiently plotted for given values of γ. Here we apply that result to the AGV plant with the largest mass value $M = 1000$kg. In Fig. 6(c) the controller parameter space is shown with the current limitation values, transient time values and the γ values.

F. Dependence on the mass value of the control current limitation and the transient time speed

All previous analysis is performed for the largest mass value $M = 1000$kg in order to obtain robust solution feasible for the total mass range. In this subsection we are interest in evaluating how conservative this solution is. Namely, we take two controllers: C_1 with $K_p = 13$ and $K_i = 95$; C_2 with $K_p = 16$ and $K_i = 150$.
C_1 is chosen among the controllers that guarantees transient time below 0.25s with $\max \Delta i \leq 8$A; C_2 is chosen so that transient time is below 0.2s with $\max \Delta i \leq 10$A.

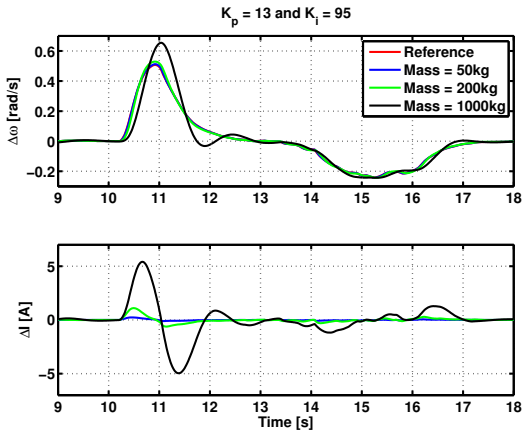

Fig. 7. Closed-loop steering speed $\Delta\omega$ in the experimental test with different loads, C_1

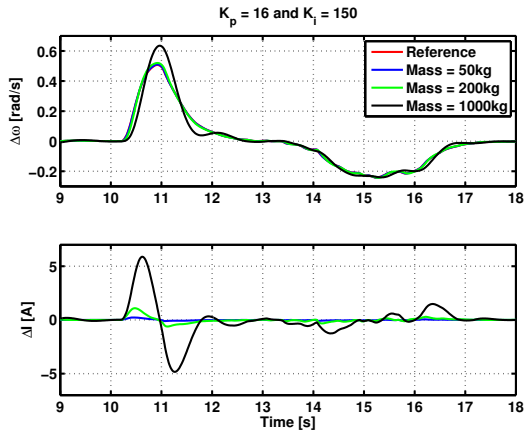

Fig. 8. Closed-loop steering speed $\Delta\omega$ in the experimental test with different loads, C_2

V. EXPERIMENTAL RESULTS

Accordingly to the parameter analysis described in Section IV, the selected controllers C_1 and C_2 have been tested on vehicle.
The vehicle has been prepared with three different operating configurations:

- no load, mass = 50kg;
- small load, mass = 200kg;
- full load mass = 1000kg.

To validate the mathematical analysis described in Section IV, a repeatable experiment has been implemented. The AGV has to follow a path composed by three pieces: a straight stretch followed by a chicane with the first left bend and then another straight stretch. In this way the steering control is well stimulated and it's possible to compare the results obtained with different loads. The longitudinal speed $\bar{\omega}^*$ is set for all the tests to 15m/min.

As can be seen in Fig. 7, the system ensures good tracking of $\Delta\omega^*$ and robustness on changes of mass. Specifically, when the mass is equal to 50kg the tracking performance is very good (the reference speed -red line- is completely hidden by the controlled output -blue line-). For higher mass values acceptable performance decrease is observed (black and green lines).

The performances of the closed loop system with the C_2 controller are shown in Fig. 8.

As can be observed, the performances of closed loop system in the second configuration (C_2) are better than the ones obtained through the first configuration. In fact, there are smaller oscillations when the AGV is fully loaded. Conversely there is a higher utilization of the control variable Δi and consequently a higher energy consumption. This is in agreement with the controller specifications that have larger current limitations in this second case. As a final remark, as evidenced by the performances achievable with both the controllers experimentally tested, the proposed method allows easy control design robust to any load condition, with clear representation of performance requirements, control limitations and H_∞ limits.

VI. CONCLUSIONS

In the paper, a magnetic guidance AGV is presented. A state space dynamical model is described in detail. In order to guarantee desirable control specifications for a wide range of possible masses ($50 < M < 1000$kg) we treat mass as uncertainty in the model. We analyze robust stability domain in the controller parameter space via randomization technique. Namely, we describe the regions of controllers satisfying control action constraints (current limitation), level sets of transient time and regions such that $||T(s)||_\infty \leq \gamma$. This approach allows us to design controller satisfying simultaneously several control objectives. For two selected controllers we make experimental tests on the vehicle and the obtained performances are in agreement with the analysis.

REFERENCES

[1] R. Tempo, G. Calafiore, and F. Dabbene, *Randomized Algorithms for Analysis and Control of Uncertain Systems*. Communications and Control Engineering Series, London: Springer-Verlag, 2004.

[2] Y. O. Y. Fujisaki and R. Tempo, "Mixed deterministic/randomized methods for fixed order controller design," vol. AC-53, no. 9, pp. 2033–2047, 2008.

[3] B. Polyak and E. Gryazina, "Hit-and-Run: New design technique for stabilization, robustness and optimization of linear systems," in *Proc. of the 17th IFAC World Congress, Seoul*, pp. 376–380, 2008.

[4] D. Arzelier, E. Gryazina, D. Peaucelle, and B. Polyak, "Mixed LMI/Randomized methods for static output feedback control design," in *Proc. of the IEEE American Control Conference*, (Baltimore), 2010.

[5] K. J. Åström and T. Hägglund, *PID Controllers*. Research Triangle Park, NC, USA: Int. Society for Measurement and Control, 1995.

[6] J. C. Alexander and J. H. Maddocks, "On the kinematics of wheeled mobile robots," *Int. J. of Robotic Research*, vol. 8, no. 5, pp. 15–27, 1989.

[7] E. Gryazina and B. Polyak, "Stability regions in the parameter space: D-decomposition revisited," *Automatica*, vol. 42, pp. 13–26, 2006.

[8] R. Smith, "Efficient Monte Carlo procedures for generating points uniformly distributed over bounded regions," *Operations Research*, vol. 32, no. 6, pp. 1296–1308, 1984.

[9] B. Polyak and E. Gryazina, "Robust stabilization via Hit-and-Run techniques," in *IEEE Multi-Conference on Systems and Control*, pp. 537–541, 2009.

[10] C. Spelta and E. Gryazina, "Describing the H_∞ set in the controller parameter space," in *Proc. of the European Control Conference*, pp. 816–823, 2007.